

# Degradation of sulfamethoxazole in water by dielectric barrier discharge plasma jet: influencing parameters, degradation pathway, toxicity evaluation

Shuheng HU (胡淑恒)<sup>1</sup>, Weiwen YAN (燕维文)<sup>1,2</sup>, Jinming YU (喻金明)<sup>1,2</sup>, Bin ZHU (朱斌)<sup>1,2</sup>, Yan LAN (兰彦)<sup>2,3</sup>, Wenhao XI (奚文灏)<sup>2</sup>, Zimu XU (许子牧)<sup>1,\*</sup>, Wei HAN (韩伟)<sup>4</sup> and Cheng CHENG (程诚)<sup>2,3,\*</sup>

<sup>1</sup> School of Resources and Environmental Engineering, Hefei University of Technology, Hefei 230009, People's Republic of China

<sup>2</sup> Institute of Plasma Physics, Chinese Academy of Sciences, Hefei 230031, People's Republic of China

<sup>3</sup> Institute of Energy, Hefei Comprehensive National Science Center, Hefei 230031, People's Republic of China

<sup>4</sup> Institute of Health and Medical Technology/Anhui Province Key Laboratory of Medical Physics and Technology, Hefei Institutes of Physical Science, Chinese Academy of Sciences, Hefei 230031, People's Republic of China

E-mail: [xzm666@hfut.edu.cn](mailto:xzm666@hfut.edu.cn) and [chengcheng@ipp.ac.cn](mailto:chengcheng@ipp.ac.cn)

Received 26 April 2022, revised 24 October 2022

Accepted for publication 25 October 2022

Published 20 January 2023



CrossMark

## Abstract

Sulfamethoxazole (SMX) is an antibiotic and widely present in aquatic environments, so it presents a serious threat to human health and sustainable development. A dielectric barrier discharge (DBD) plasma jet was utilized to degrade aqueous SMX, and the effects of various operating parameters (working gas, discharge power, etc) on SMX degradation performance were studied. The experimental results showed that the DBD plasma jet can obtain a relatively high degradation efficiency for SMX when the discharge power is high with an oxygen atmosphere, the initial concentration of SMX is low, and the aqueous solution is under acidic conditions. The reactive species produced in the liquid phase were detected, and OH radicals and O<sub>3</sub> were found to play a significant role in the degradation of SMX. Moreover, the process of SMX degradation could be better fitted by the quasi-first-order reaction kinetic equation. The analysis of the SMX degradation process indicated that SMX was gradually decomposed and 4-amino benzene sulfonic acid, benzene sulfonamide, 4-nitro SMX, and phenylsulfinyl acid were detected, and thus three possible degradation pathways were finally proposed. The mineralization degree of SMX reached 90.04% after plasma treatment for 20 min, and the toxicity of the solution fluctuated with the discharge time but eventually decreased.

Keywords: dielectric barrier discharge (DBD) plasma jet, sulfamethoxazole (SMX), degradation, pathway, toxicity

(Some figures may appear in colour only in the online journal)

## 1. Introduction

Environmental endocrine disruptors refer to exogenous substances that affect the endocrine system. As a category of

burgeoning environmental contaminants, they present a serious threat to human health and sustainable development [1, 2]. Sulfamethoxazole (SMX), a sulfonamide antibiotic, is a typical endocrine disruptor [3, 4], and it is widely used in animal feed and human medicine due to its broad spectrum and relatively strong antimicrobial activity [5]. To date, SMX

\* Authors to whom any correspondence should be addressed.

has been constantly detected in wastewater, reclaimed water, surface water and even drinking water in many countries [6–10]. As a persistent organic pollutant, it is difficult for SMX to be completely degraded by conventional sewage treatment methods, leading to its further enrichment in aqueous environments. Therefore, SMX has also been detected in water sediments and aquatic organisms through biosorption and bioaccumulation, which has led to the production of antibiotic-resistant bacteria and antibiotic-resistant genes [8–10].

The conventional methods of degrading SMX include biological, physical and chemical approaches. Unfortunately, SMX has a strong antibacterial effect on acidogenic and methanogenic bacteria, so it is very hard to remove from aqueous solution by biodegradation processes. According to the research of Rosal *et al* [11], the removal rate of SMX from wastewater is less than 20% by the traditional activated sludge method. It is well known that the degradation efficiency of the membrane bioreactor is higher than that of the traditional activated sludge method, but its degradation efficiency for SMX is still low [12]. Although the physical adsorption is easy to remove pollutants from wastewater, it is only a temporary removal method and cannot completely degrade the pollutants in aqueous solution. Therefore, the application of the adsorption method carries the risk of secondary pollution. In addition, the cost of the adsorbents and the complex wastewater environment in the actual application limit the removal of SMX by the adsorption method. The chemical methods of degrading SMX include photocatalysis, ozonation, electrochemical oxidation, etc, but these methods are either time-consuming or have low mineralization rates [13–15]. Therefore, a highly efficient, green and environmentally friendly method to degrade or completely remove SMX from wastewater is desperately needed.

Fortunately, non-thermal plasma (NTP) has gradually entered public awareness and attracted widespread attention. As a novel advanced oxidation process, NTP has been widely applied in the inactivation of bacteria, surface modification, contaminant removal [16–18], etc. NTP is generated by electrical discharge in the gas phase or gas-liquid interface, leading to the emergence of ultraviolet light and reactive species in liquid, such as long-lived species ( $\text{H}_2\text{O}_2$ ,  $\text{O}_3$ ,  $\text{NO}_3^-$ , etc) and short-lived species ( $\cdot\text{OH}$ ,  $\cdot\text{O}_2^-$ , hydrated electron, etc), which are shown to play an important role in removing refractory organic pollutants [19, 20]. Dielectric barrier discharge (DBD) is a common form of discharge to generate NTP, and it has been widely used due to its simple reaction conditions, good discharge stability and high treatment efficiency, and it has great potential in the removal of biorefractory organic matter in wastewater [21]. Kim *et al* [22] applied a non-thermal DBD plasma reactor for the removal of three kinds of sulfonamide antibiotics in water and the target pollutants were almost completely removed, but the total organic carbon (TOC) removal efficiency was found to be no more than

40% after 60 min of discharge treatment. Various catalysts have been used to promote the generation of reactive species in the plasma system for the purpose of further improving the plasma treatment efficiency. Deng *et al* [23] investigated the degradation effect on diclofenac by a DBD plasma-catalyst system and founded that 45.8% decomposition of diclofenac was achieved with DBD alone while 96.4% degradation of diclofenac was attained with DBD combined with nano- $\text{Fe}^0\text{-CeO}_2$  composites. Although the use of catalysts can enhance the efficiency of the DBD plasma for pollutant degradation, the addition of catalysts usually comes with additional costs and recovery steps.

Combining plasma discharges with bubble generation provides a train of thought for increasing degradation performance. Liu *et al* [24] used a DBD/bubble reactor to degrade aniline in aqueous solution and found that the degradation effect of aniline by the combined DBD with bubbles was better than its counterpart that did not use bubbles. A plasma jet is an effective technique for the removal of stable organic pollutants present in wastewater [25], and Rashid *et al* [26] explored the treatment effect of a plasma jet on textile wastewaters by utilizing an atmospheric pressure air discharge plasma jet and achieved a degradation rate of almost 70% within 10 min of treatment. Therefore, the aim of this research was to design a DBD plasma jet to degrade the refractory pollutant SMX in aqueous solution, with the flow of the working gas transporting the gas phase reactive species in the form of bubbles to the aqueous solution via underwater micro-holes during the discharge. For this purpose, the effects of working gas, discharge power, initial concentration of SMX, and initial pH of the solution were studied. Then, the roles of reactive species ( $\cdot\text{OH}$ ,  $\text{O}_3$ ,  $\text{H}_2\text{O}_2$ ) in SMX degradation were investigated. Finally, the SMX degradation process (kinetic model, TOC, degradation intermediates and pathways, and toxicity evaluation) was explored.

## 2. Material and methods

### 2.1. Materials

SMX ( $\text{C}_{10}\text{H}_{11}\text{N}_3\text{O}_3\text{S}$ , purity  $\geq 98\%$ ) was purchased from Beijing Solarbio Technology Co., Ltd. Methanol and acetonitrile (HPLC grade) were purchased from Sigma-Aldrich. Formic acid (LCMS/HPLC grade) was purchased from Anaqua Chemicals Supply. Hydrochloric acid and sodium hydroxide were obtained from Sinopharm Chemical Reagent Co., Ltd. All solutions used in this work were prepared from ultrapure water.

### 2.2. Experimental setup

Figure 1 shows a schematic of the DBD plasma jet apparatus driven by an AC high voltage power supply. The device can be divided into two parts: the DBD plasma jet reactor and the ozone reuse reactor. The DBD plasma jet reactor was the discharge occurrence zone and was accompanied by the

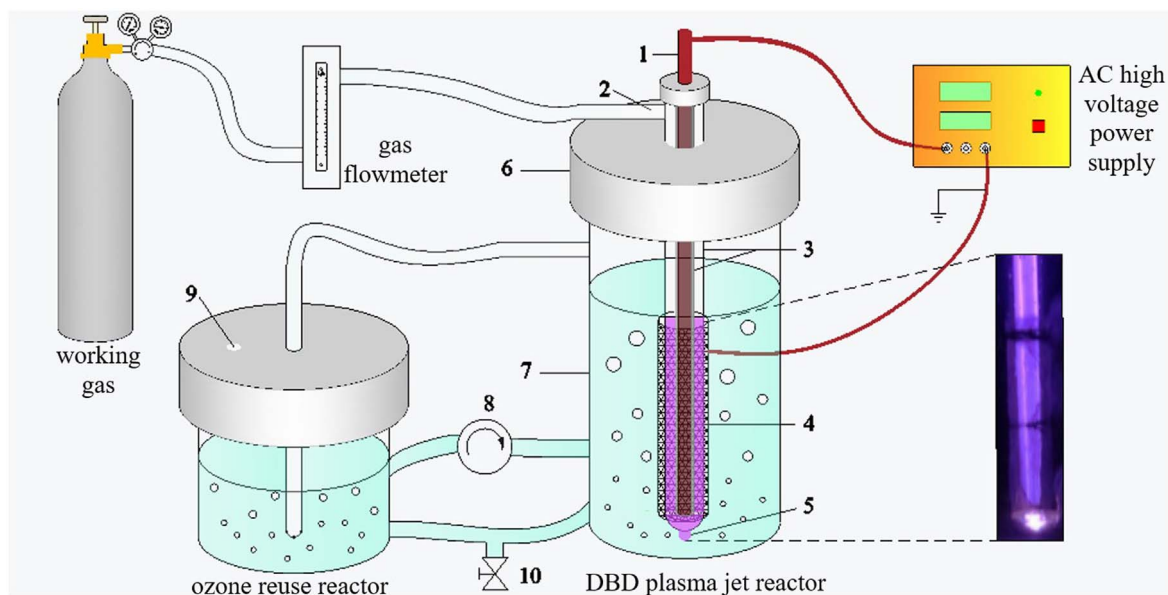


**Figure 1.** Schematic of the DBD plasma jet apparatus (1 high voltage electrode, 2 gas inlet, 3 quartz glass tube, 4 ground electrode, 5 plasma jet, 6 polytetrafluoroethylene, 7 glass tube, 8 peristaltic pump, 9 gas outlet, 10 sampling port).

generation of plasma; a copper rod with a diameter of 2 mm served as a high-voltage electrode and was tightly wrapped by a quartz glass tube with an inner diameter of 2 mm and an outer diameter of 4 mm. The outer wall of another quartz glass tube (inner diameter of 6 mm; outer diameter of 8 mm) was wrapped with a layer of stainless-steel mesh, which served as a ground electrode. The working gas passed through the gap between the two glass tubes at a flow rate of  $2 \text{ l min}^{-1}$  and generated plasma discharges under the excitation of high voltage. The ozone reuse reactor was mainly to further utilize the ozone produced in the DBD plasma jet reactor. At the time of discharge, 200 ml of SMX solutions with different concentrations were prepared with ultrapure water, and a peristaltic pump (YZ1515x) was used to circulate the solution between the DBD plasma jet reactor and the ozone reuse reactor to guarantee that their solution volumes were 160 ml and 40 ml, respectively.

### 2.3. Analytical methods

The plasma discharge voltage and current were recorded by a high-voltage probe and a current probe with an oscilloscope, and the plasma discharge power was calculated using Lissajous's graphic method. Thereafter, the output power was calculated as follows (equation (1)) [27]:

$$P = \frac{1}{T} \int_0^T UI dt = \frac{C}{T} \int_0^T U \frac{dU_c}{dt} dt = fC \oint U dU_c = fCS \quad (1)$$

where  $P$  (W) is the output power,  $U$  (V) is the output voltage,  $I$  (A) is the output current,  $U_c$  (V) is the sampling capacitor voltage,  $f$  (Hz) is the frequency,  $C$  (F) is the capacitance, and  $S$  is the area of the Lissajous figure.

The SMX concentrations in a water sample were measured by HPLC (high performance liquid chromatography, Agilent 1260), and the sample solution was filtered through a

$0.22 \mu\text{m}$  polyethersulfone syringe filter before testing. The chromatographic column was a Hypersil ODS2 C18 column ( $5 \mu\text{m}$ ,  $4.6 \text{ mm} \times 150 \text{ mm}$ ), working at a temperature of  $30 \text{ }^\circ\text{C}$ . The mobile phase consisted of 60% ultrapure water and 40% acetonitrile at a flow rate of  $1 \text{ ml min}^{-1}$ . The volume of the sample injection and detector wavelength were  $20 \mu\text{l}$  and  $280 \text{ nm}$ , respectively. The degradation efficiency for SMX was calculated as indicated in equation (2):

$$\eta = \left(1 - \frac{C_t}{C_0}\right) \times 100\% \quad (2)$$

where  $C_0$  ( $\text{mg l}^{-1}$ ) is the SMX initial concentration,  $C_t$  ( $\text{mg l}^{-1}$ ) is the SMX concentration at treatment time  $t$ , and  $\eta$  (%) is the degradation efficiency.

The energy yield was used to indicate the amount of SMX that can be degraded per unit of energy consumed during the DBD plasma jet process (equation (3)) [28]:

$$Y = \frac{60 \times C_0 V \eta}{1000 \times Pt} \quad (3)$$

where  $Y$  ( $\text{g (kWh)}^{-1}$ ) is the energy yield,  $V$  (l) is the solution volume, and  $t$  (min) is the discharge time.

The concentrations of the long-lived reactive species  $\text{O}_3$  and  $\text{H}_2\text{O}_2$  in the plasma treatment solution were measured using a spectrophotometer (photoLab 7100 VIS, WTW), and the detection kits were 00607 and 18789, respectively. The OH radical can be trapped by non-fluorescent terephthalic acid (TA) to generate 2-hydroxyterephthalic acid (HTA) with intense fluorescence at an excitation wavelength of  $310 \text{ nm}$  and an emission wavelength of  $425 \text{ nm}$  [29], and thus the formation rate of the short-lived reactive species OH radical in aqueous solution can be indirectly described by the concentration of HTA detected.

In order to understand the degradation process of SMX by DBD plasma jet, the experimental data were fitted using the quasi-first-order reaction kinetic equation as follows

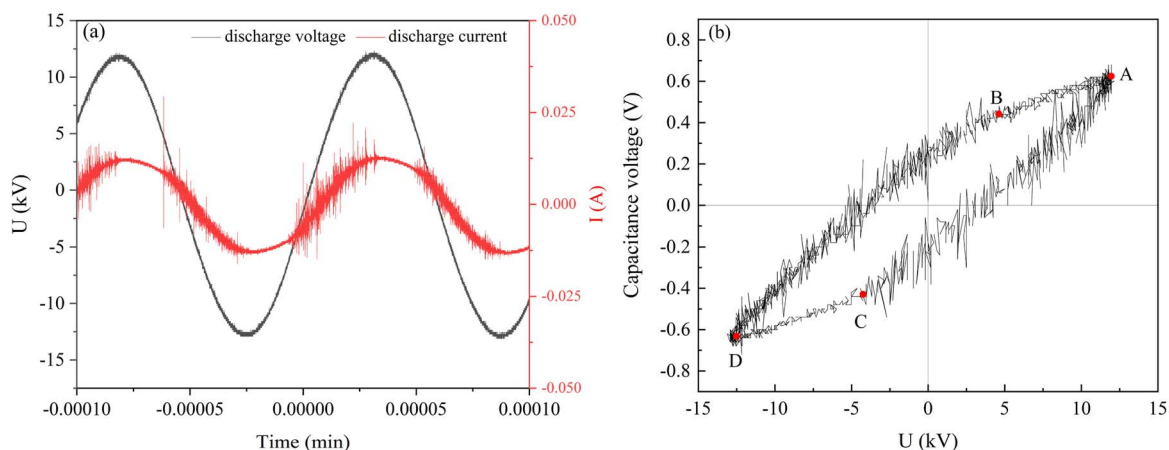


Figure 2. (a) The voltage-current waveform of DBD plasma jet at 22.85 W, (b) Lissajous figures of DBD plasma jet at 22.85 W.

(equation (4)):

$$\ln\left(\frac{C_0}{C_t}\right) = kt \tag{4}$$

where  $k$  ( $\text{min}^{-1}$ ) is the reaction rate constant.

The intermediate products of SMX degradation were analyzed using an ultraperformance liquid chromatography time-of-flight mass spectrometer (UPLC-MS, LCT Premier XE, Waters). The mobile phase A was acetonitrile, and the mobile phase B was 0.1% formic acid in water. The samples to be processed were subjected to gradient elution with mobile phases A and B at a flow rate of  $0.5 \text{ ml min}^{-1}$ : 10% mobile phase A was held for 0.2 min, then linearly increased to 95% from 0.2 to 4.7 min, maintained for 0.5 min, and finally decreased linearly to 10% from 5.2 to 7.2 min. Data were analyzed by MassLynx 4.1 software. The concentration of TOC was measured using a TOC survey meter (multi N/C 3100, analytikjena).

The toxicity of the sample solution was evaluated using *Escherichia coli* (*E. coli*) according to the method of Mirzaei et al [30]. After plasma treatment for different times, 0.5 ml of the sample solution and 0.5 ml of Lysogeny broth medium were thoroughly mixed in a centrifuge tube, and then 0.125 ml ( $1 \times 10^8 \text{ CFU ml}^{-1}$ ) *E. coli* was added to each tube and incubated at  $37 \text{ }^\circ\text{C}$  and  $200 \text{ r min}^{-1}$ . After 3 h, the absorbance value of each sample at 600 nm was measured using a spectrophotometer. The growth inhibition rate of *E. coli* was used to represent the toxicity of the solution, and it could be calculated according to equation (5):

$$I = \frac{A_0 - A}{A_0} \times 100\% \tag{5}$$

where  $I$  is the inhibition rate, and  $A$  and  $A_0$  are the absorbances of the treated group and the control group (0.5 ml of sterile water instead of 0.5 ml of sample solution), respectively. In addition, the aquatic toxicity of SMX and its degradation intermediates was predicted with the aid of ECOSAR 2.0 software.

### 3. Results and discussion

#### 3.1. Discharge properties

The efficiency of the DBD plasma jet in degrading pollutants is closely related to the discharge power. Figure 2(a) displays the discharge voltage and current changes over 1.8 cycles at a peak voltage of 12.14 kV and a peak current of 0.02 A. Figure 2(b) is the Lissajous figure obtained relying on the sampling capacitor at the same time. It is clear that this Lissajous figure is approximately a parallelogram with four vertices A, B, C, and D, and points A to B or points D to C represent the power supply charging process when discharge is extinguished. Points A to C or point Ds to B indicate the discharge process, during which plasma is generated. According to the Lissajous figure, the discharge power (22.85 W) in one cycle can be calculated based on equation (1).

#### 3.2. Degradation efficiency of SMX under different operating parameters

##### 3.2.1. Influence of working gas on SMX degradation.

Figure 3(a) displays the degradation efficiency of SMX in aqueous solution by DBD plasma jet when oxygen and air were used as the working gas. The discharge power was 38.12 W, the initial concentration of SMX solution was  $20 \text{ mg l}^{-1}$ , and the initial pH of solution was 5.40. When air was used as the working gas, the degradation efficiency of SMX was improved from 38.98% to 98.48% as the treatment time is extended from 5 min to 30 min. In comparison, a higher degradation efficiency was achieved when oxygen was used as the working gas, and the degradation efficiency reached 99.50% after 5 min of plasma treatment. This may be due to the fact that the liquid phase OH induced by plasma is also an important factor in the degradation of organic pollutants in water. Our previous studies have shown that the generation rate of liquid OH induced by oxygen plasma in water is much greater than that of air plasma [31]. In addition, the ozone generated by the oxygen plasma jet is much larger than the air plasma jet when they are operated at the same

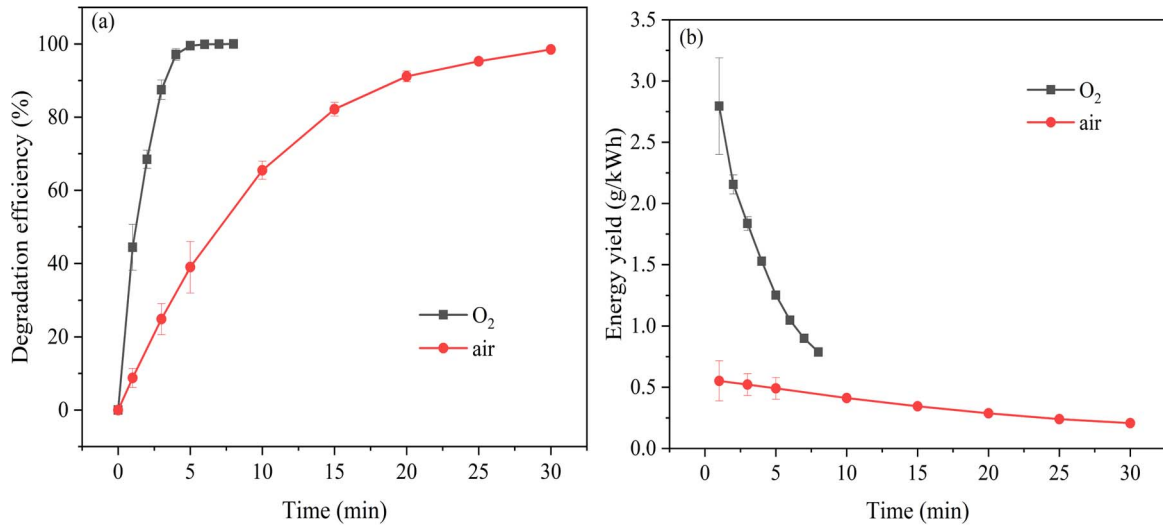


**Figure 3.** The effect of working gas type (O<sub>2</sub> and air) on (a) degradation efficiency and (b) energy yield of SMX in plasma system.

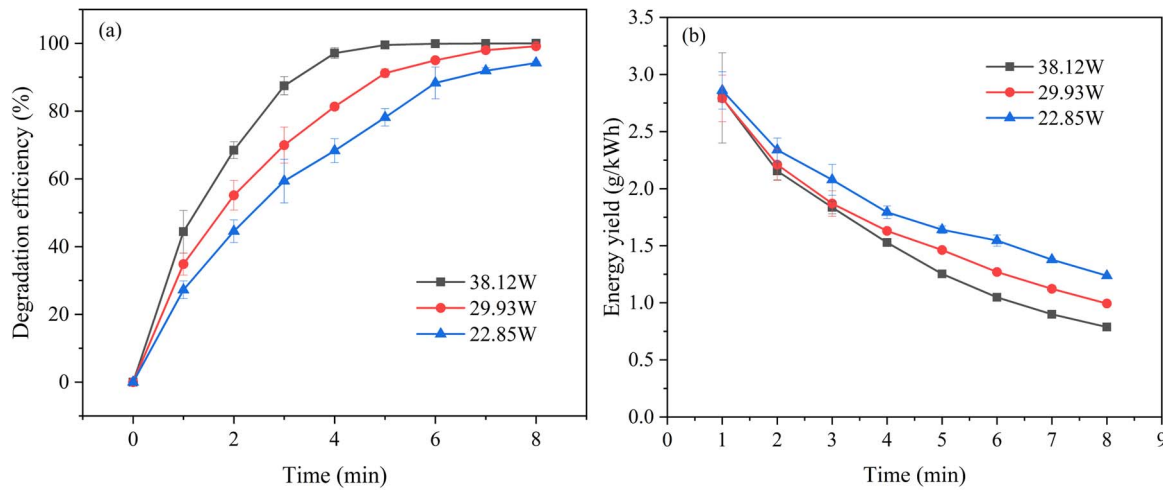
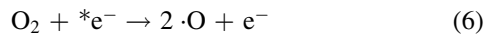


**Figure 4.** The effect of discharge power on (a) degradation efficiency and (b) energy yield of SMX in plasma system.

power. According to reaction reactions (6) and (7) [32–34], the oxygen atoms and electrons are important intermediates for ozone production. The air also contains other components such as nitrogen, which will quench some of the electrons to form nitrogen atoms and further consume oxygen atoms to form nitroxides [35]. For this reason, air plasma produces less ozone than oxygen plasma.



Therefore, these reasons are that the degradation efficiency of oxygen plasma on SMX is significantly higher than that of air plasma. Figure 3(b) shows the energy yield of oxygen and air plasma to degrade SMX. After 1 min of discharge treatment, the energy efficiencies of oxygen and air plasma were 2.79 g (kWh)<sup>-1</sup> and 0.55 g (kWh)<sup>-1</sup>, respectively. This also indicates that degrading the same amount of SMX, the air plasma will consume more energy. Based on

these results, later experiments were all carried out with oxygen as the working gas.

### 3.2.2. Influence of discharge power on SMX degradation.

The discharge power is a very important factor in the degradation of organic pollutants because it is closely related to the formation of reactive species. Figure 4(a) displays the influence of the discharge power on SMX degradation. The initial concentration of SMX solution was 20 mg l<sup>-1</sup>, and the initial pH of solution was 5.40. After 5 min of oxygen plasma treatment, the degradation efficiency of SMX increased to 78.12% when the discharge power was 22.85 W. The removal performance was further increased with the promoted discharge power. When the discharge power increased to 29.93 W and 38.12 W, the degradation efficiency of SMX reached 91.19% and 99.50%, respectively. This may be due to the fact that more reactive species would be generated at relatively higher discharge power, and thus stronger SMX degradation performance was observed at higher discharge power in this study. Figure 4(b) displays the variation that the

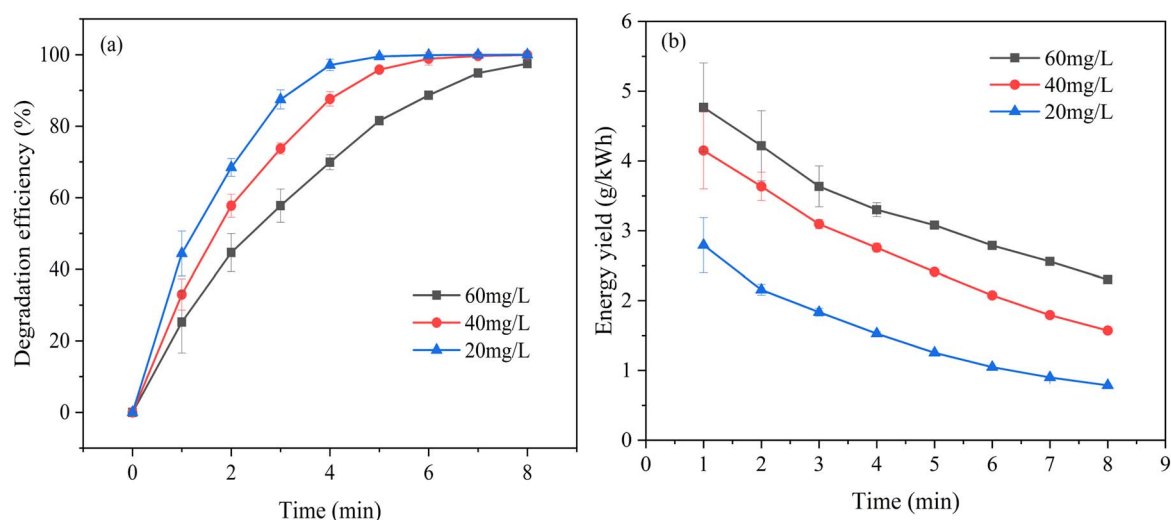


**Figure 5.** The effect of initial concentration on (a) degradation efficiency and (b) energy yield of SMX in plasma system.

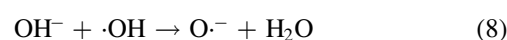
energy yield of DBD plasma jet to degrade SMX under different discharge powers. With the extension of discharge time, SMX was gradually degraded by oxygen plasma. Therefore, under the condition of the same discharge power, there is less and less SMX that can react with the reactive species, so the energy yield gradually decreases with discharge time. The energy yield also varies among different discharge powers. After 5 min of discharge treatment, the energy yield decreased from  $1.64 \text{ g (kWh)}^{-1}$  at  $22.85 \text{ W}$  to  $1.25 \text{ g (kWh)}^{-1}$  at  $38.12 \text{ W}$ . Higher power instead results in slightly lower energy utilization, which may be mainly due to the fact that the increased discharge powers led to more energy lost in the form of heat energy. This experimental result indicated that it was difficult to obtain the best degradation efficiency and higher energy yield simultaneously. In order to achieve higher degradation efficiency, later experiments were all carried out at the discharge power of  $38.13 \text{ W}$ .

**3.2.3. Influence of initial concentration of SMX on its degradation.** The concentration of SMX may vary greatly in actual wastewater, which may have a serious influence on the degradation efficiency of SMX in aqueous solution by DBD plasma jet. Therefore, the effect of initial concentration of SMX on degradation efficiency is not something that can be neglected. Figure 5(a) displays the degradation efficiency as a function of discharge time at different initial concentrations of SMX. After 5 min of discharge treatment, the degradation efficiencies of SMX with initial concentrations of  $60 \text{ mg l}^{-1}$ ,  $40 \text{ mg l}^{-1}$  and  $20 \text{ mg l}^{-1}$  were  $81.52\%$ ,  $95.81\%$  and  $99.50\%$ , respectively. Relatively higher degradation efficiency was observed at lower concentration, which may be mainly attributed to the fact that the quantity of generated reactive species was a constant value when the discharge power was the same value. Therefore, the greater the initial concentration of SMX, the less reactive species per unit mass of SMX is available. In addition, higher

concentration of SMX might generate more intermediate products to consume active substances, which leads to a further reduction in the efficiency of SMX degradation. Figure 5(b) displays the variation that the energy yield of DBD plasma jet to degrade SMX under different initial concentrations of SMX. After 5 min of discharge treatment, the energy yield increased from  $1.25 \text{ g (kWh)}^{-1}$  at  $20 \text{ mg l}^{-1}$  to  $3.08 \text{ g (kWh)}^{-1}$  at  $60 \text{ mg l}^{-1}$ . Although the reactive species that could be utilized were not sufficiently abundant at higher initial SMX concentrations, higher concentrations of SMX would cause a more intense competition of SMX molecules for reactive species, resulting in increased energy yield.

#### 3.2.4. Influence of initial pH of solution on SMX degradation.

The initial pH value of solution is not only a very important water quality indicator, but also affects the removal efficiency of pollutants in wastewater [36], so it is necessary to determine the effect of the initial pH of solution on the degradation efficiency of SMX by DBD plasma jet. Figure 6(a) displays the degradation efficiency as a function of discharge time at different initial pH values of solution. After 5 min of plasma treatment, the degradation efficiencies reached  $99.68\%$ ,  $99.50\%$ ,  $93.88\%$ , and  $84.94\%$  at the initial pH values of  $3.04$ ,  $5.40$ ,  $7.03$  and  $10.33$ , respectively. Relatively higher degradation efficiency was observed at lower the initial pH value, which may be caused by the following two aspects. On one hand, plasma produces a lot of reactive species, such as OH radicals and  $\text{O}_3$ , which possess high oxidation potential in acidic condition [37]. However, in an alkaline environment, the OH radicals generated by DBD plasma jet may be consumed by  $\text{OH}^-$  (reaction (8)), which greatly reduces the number of OH radicals [38, 39].



On the other hand, SMX dissociation constants are  $\text{pK}_{a1}$  of  $1.7$  and  $\text{pK}_{a2}$  of  $5.6$  [40], so it is highly dissociated deprotonated form at the initial pH values of  $7.03$  and  $10.33$ .

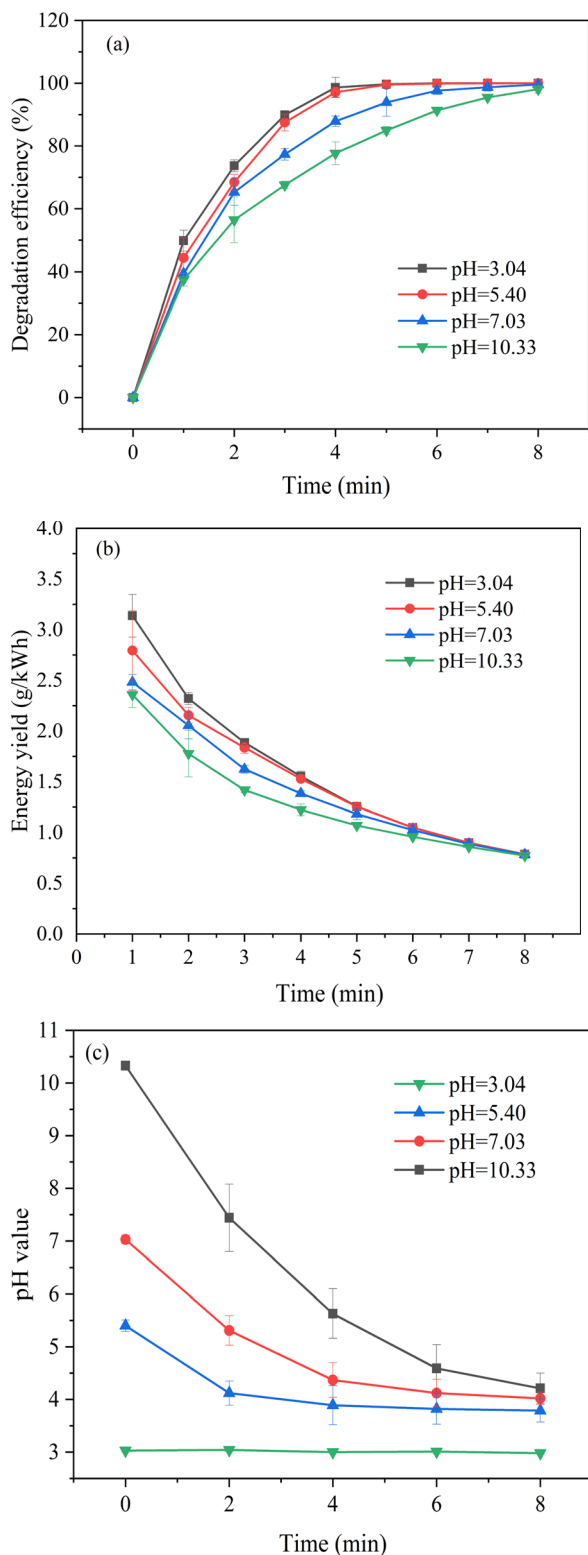


**Figure 6.** The effect of initial pH on (a) degradation efficiency and (b) energy yield of SMX in plasma system. (c) pH value changes with discharge time.

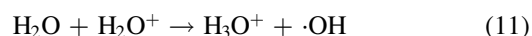
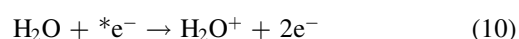
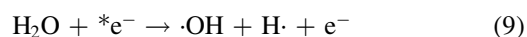
Nevertheless, SMX neutral form are dominant at pH values of 3.04 and 5.40. Some studies have reported that the mass transfer coefficient of neutral form was higher than deprotonated form [41–43]. Therefore, the mass transfer efficiency in acidic environment is higher than that in alkaline

environment, which may have contributed to the higher efficiency of SMX degradation at lower pH. Moreover, the pH value of SMX solution was measured during the plasma treatment process, and it decreased gradually with the amplification of the treatment time as shown in figure 6(c). The pH value drop may be attributed to the ionization of water molecules to produce  $\text{H}_3\text{O}^+$  (reactions (10) and (11)) [31, 44], which also seems to be more conducive to the degradation of SMX. Relatively higher degradation efficiency in acidic condition also leads to higher energy yield. As shown in figure 6(b), the energy yields of SMX solution with initial pH values of 3.04, 5.40, 7.03 and 10.33 were  $1.26 \text{ g (kWh)}^{-1}$ ,  $1.25 \text{ g (kWh)}^{-1}$ ,  $1.18 \text{ g (kWh)}^{-1}$ , and  $1.07 \text{ g (kWh)}^{-1}$ , respectively, after 5 min of discharge treatment. In conclusion, although the removal effect was slightly better at pH 3.04 than that at pH 5.40, the latter experiments were all carried out at pH 5.40 because the medium of pH 5.40 is more moderate.

### 3.3. Detection of reactive species for SMX degradation

**3.3.1. Optical emission spectra of oxygen plasma.** There will be atoms of excited states generated in the process of DBD plasma jet, which are important intermediates for the generation of reactive species in aqueous solution. The optical emission spectra of these high-energy atoms were examined by a fiber-optic spectrometer (Maya2000Pro). Figure 7(a) displays the optical emission spectra of oxygen plasma in the range of 450–900 nm. It is obvious that the highest intensity emission peaked at 777.4 nm, corresponding to the O I. Optical emission peaks of O I were also observed at 798.3 nm and 844.6 nm.

**3.3.2. Role of OH radicals.** Hydroxyl radical is a strong oxidizing reactive species that can be produced by DBD plasma jet. Previous studies reported that OH radicals could well degrade SMX in aqueous solution [45–47]. As shown in figure 7(b), the concentrations of OH radicals in aqueous solution reached  $5.06 \mu\text{M}$  after 4 min of plasma treatment. Water molecules can not only directly generate OH radicals through electron dissociation (reaction (9)) [48], but also are ionized and excited to produce the  $\text{H}_2\text{O}^+$  followed by a reaction with other molecules to generate  $\text{H}_3\text{O}^+$  and OH radicals (reactions (10) and (11)) [44]. In addition, when oxygen was used as the working gas, the active oxygen atoms formed by the dissociation of oxygen molecules could react with water molecules to generate OH radicals in the gas phase (reactions (6) and (12)) [32].



In addition, the concentration of OH radicals in aqueous solution showed an almost linear increase trend with the treatment time, and the productive rate of OH radicals is

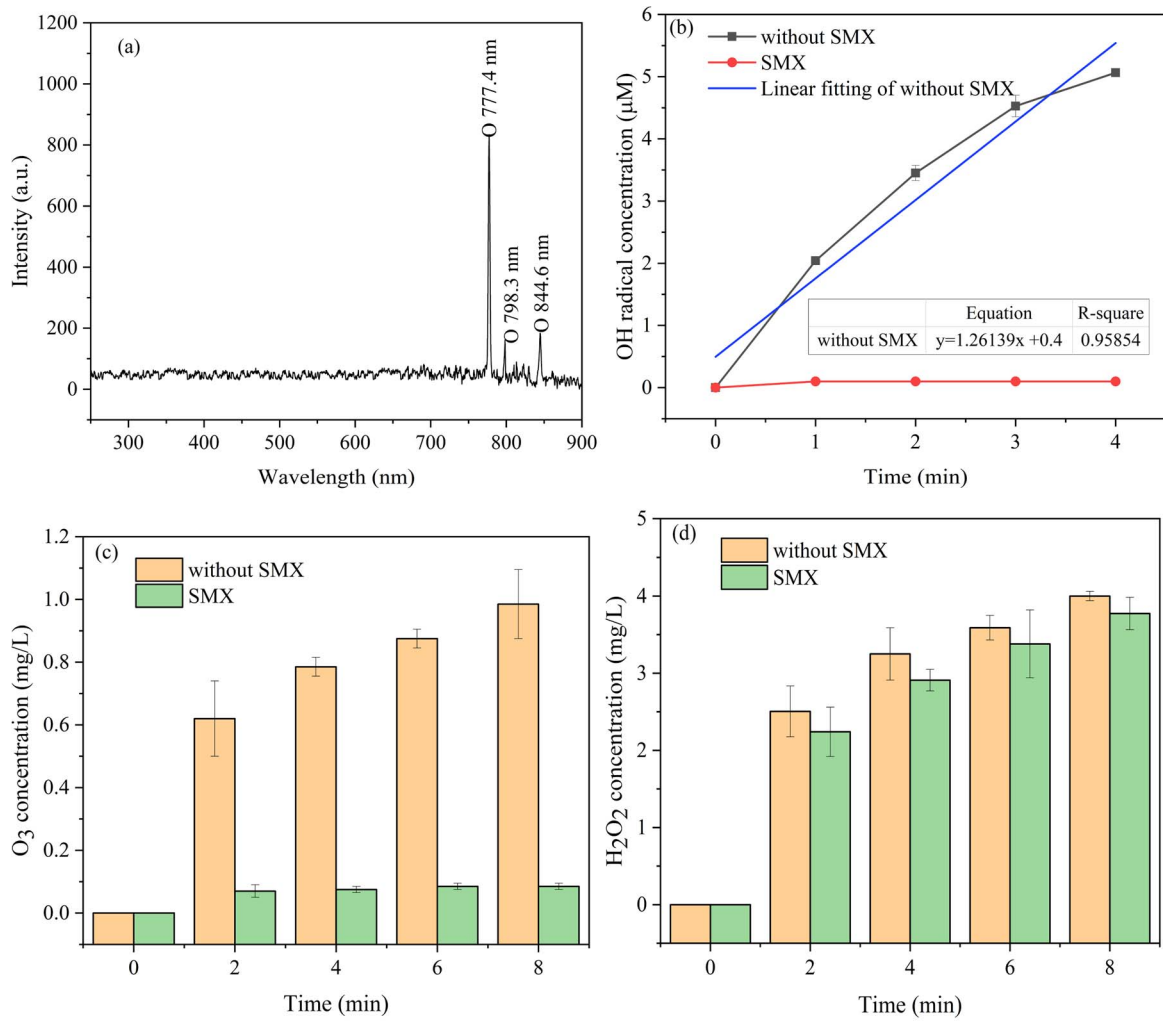


**Figure 7.** Detection of reactive species in DBD plasma jet apparatus. (a) Optical emission spectra, (b) OH radical concentration in the presence and absence of SMX, (c) O<sub>3</sub> concentration in the presence and absence of SMX, (d) H<sub>2</sub>O<sub>2</sub> concentration in the presence and absence of SMX.

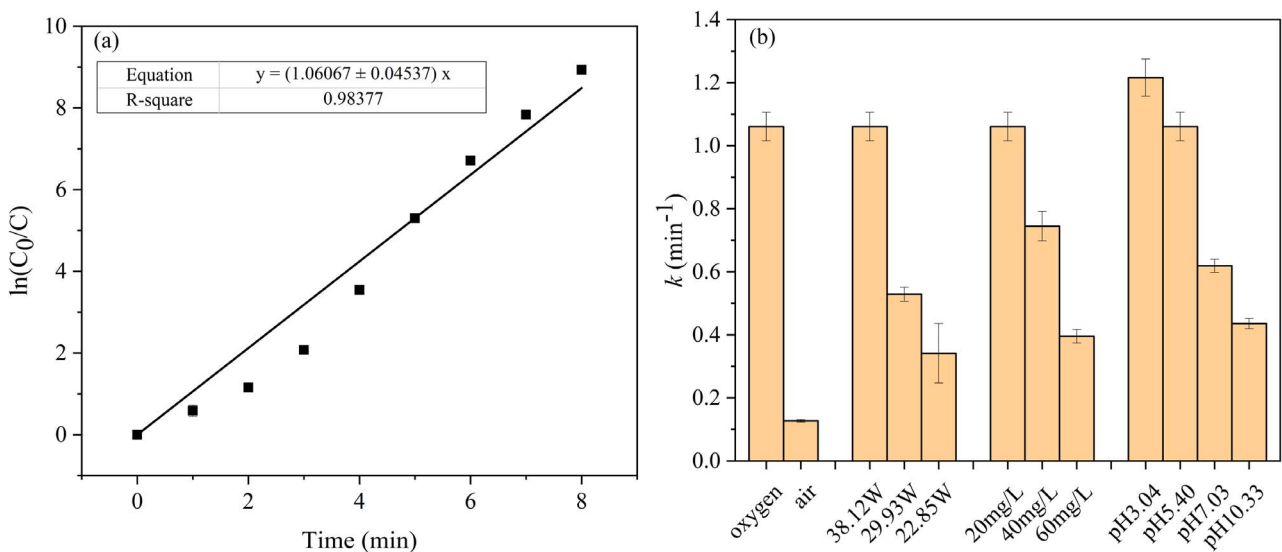


**Figure 8.** (a) Quasi-first-order kinetic model of SMX degradation (oxygen plasma, discharge power of 38.12 W, initial SMX concentration of 20 mg l<sup>-1</sup>, initial pH 5.40), (b) rate constants ( $k$ ) under different experimental parameters.



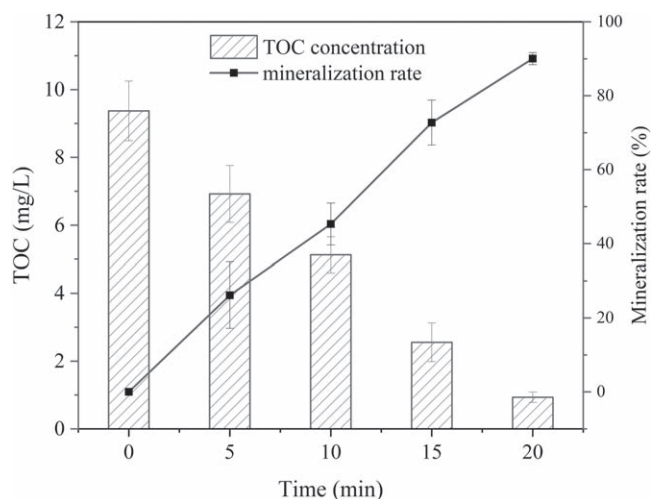


**Figure 9.** Changes in TOC concentration and mineralization rate with discharge time.

$2.1 \times 10^{-8} \text{ M s}^{-1}$ . Whereas, the concentration of OH radicals detected decreased after 4 min (data not shown). This phenomenon may be that there was no enough TA in the solution to capture OH radicals after 5 min of plasma treatment, which causes the detected HTA to decrease instead. Furthermore, the decomposition of HTA by excess OH radicals and other reactive species has to be considered [31, 49]. The concentration of OH radicals mentioned above was measured in ultrapure water, while it dropped to almost zero when SMX was present in water. This may be due to the distinct advantage of SMX in competing with TA for OH radicals in water, so the reaction between TA and OH radicals is limited, resulting in that we did not detect HTA in the presence of SMX. These results indicate that OH radicals play a vital role in the degradation process of SMX DBD plasma jet.

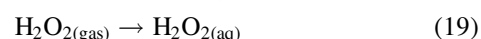
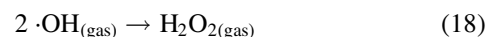
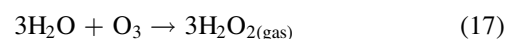
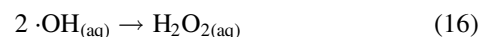
**3.3.3. Role of  $O_3$ .** Ozone is a strong oxidizing reactive species that can be produced in a DBD plasma jet. Figure 7(c) shows that the concentration of  $O_3$  in ultrapure water gradually increased with the discharge time and reached  $0.98 \text{ mg l}^{-1}$  after 8 min of treatment.  $O_3$  dissolved in water produces OH radicals through radical chain reactions (reactions (13)–(15)) [2], which also seems to prove that more OH radicals would be generated under acidic conditions and in turn lead to more efficient degradation of SMX.



However, the concentration of  $O_3$  in water only increased to  $0.09 \text{ mg l}^{-1}$  in the presence of SMX. The concentration of dissolved ozone in water in the absence of SMX was more than ten times higher than that in its presence. The results showed that the conversion of  $O_3$  into OH radicals may be limited and insufficient for the degradation of SMX. At the same time, it can also be illustrated that the degradation of

SMX by  $O_3$  may be attributed to the direct reaction of ozone and SMX. Several studies have also shown that  $O_3$  could selectively attack the functional groups of SMX, such as aromatic rings and double bonds [13, 50], to realize the direct oxidative degradation of SMX. In summary,  $O_3$  was a crucial reactive species for SMX degradation in this research.

**3.3.4. Role of  $H_2O_2$ .** Figure 7(d) shows that the concentration of  $H_2O_2$  in ultrapure water gradually increased with the discharge time and reached  $4 \text{ mg l}^{-1}$  after 8 min of treatment.  $H_2O_2$  generated by the combination reaction of liquid-phase OH radicals and the dissolution of gaseous  $H_2O_2$  have the potential to be sources of aqueous  $H_2O_2$ . The combination reaction of aqueous OH radicals was considered to be an important approach for producing  $H_2O_2$  (reaction (16)) [44]. The above experimental results indicate that almost no OH radicals remained in water in the presence of SMX (figure 7(b)), at which point  $H_2O_2$  should be correspondingly absent or rarely present in aqueous solution. However, the concentration of  $H_2O_2$  in SMX solution also gradually increased with the discharge time and reached  $3.78 \text{ mg l}^{-1}$  after 8 min of treatment, so the results indicate that the combination of aqueous OH radicals is not a major source of  $H_2O_2$ . Therefore, the dissolution of gaseous  $H_2O_2$  (reaction (19)) may play a regnant role in the production of aqueous  $H_2O_2$  by DBD plasma jet, and Chen *et al* also found that the aqueous  $H_2O_2$  is mainly from the dissolution of gaseous  $H_2O_2$  in the helium plasma jet [51]. The main  $H_2O_2$  generation reactions in the gas phase are shown in reactions (17) and (18) [44, 52].



Unlike OH radicals and  $O_3$ , the concentration of  $H_2O_2$  decreased particularly little when SMX was present in aqueous solution, which indicates that  $H_2O_2$  in aqueous solution has no obvious effect on the degradation of SMX. However, the above results indicate the crucial role of OH radicals for SMX degradation, and thus we conclude that the photolysis of  $H_2O_2$  is not a source of OH radicals in aqueous solution in a DBD plasma jet system, so the reaction represented by reaction (20) has a low probability of occurring in this research, which was also demonstrated by Park *et al* [53]. To sum up, the effect of the long-lived component  $H_2O_2$  in aqueous solution generated by a DBD plasma jet on the degradation of SMX is insignificant.

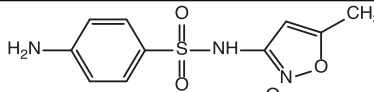
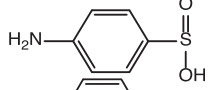
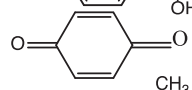
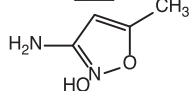
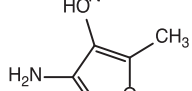
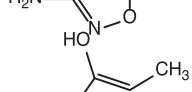
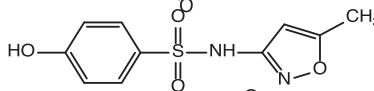
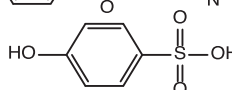
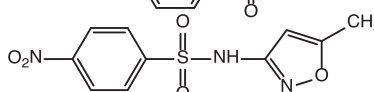
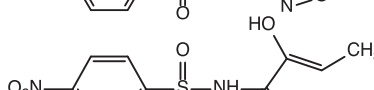
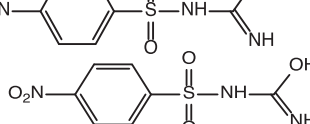
### 3.4. SMX degradation process

**3.4.1. Kinetic analysis of SMX degradation.** Figure 8(a) displays that the variation in  $\ln(C_0/C_t)$  with discharge time under the optimal degradation conditions obtained above (oxygen plasma, discharge power of 38.12 W, initial

**Table 1.** Comparison of the removal rate of TOC during SMX degradation by different approaches.

Approaches	[SMX] <sub>0</sub> (mg l <sup>-1</sup> )	Time (min)	TOC removal rate (%)	References
Gamma radiation/Fenton-like oxidation	20	70	26.7	[54]
Peroxymonosulfate oxidation	25	14	47.0	[55]
Electrochemical oxidation	50	240	77.0	[15]
UV/peroxydisulfate oxidation	10	120	91.0	[56]
DBD	50	60	24.3	[22]
DBD plasma jet	20	20	90.0	This research

**Table 2.** Mass-to-charge ratios of intermediates and the corresponding deduced chemical formulas.

Product	Chemical formula	Ionization mode	<i>m/z</i>	Structural formula
SMX	C <sub>10</sub> H <sub>11</sub> O <sub>3</sub> N <sub>3</sub> S	ESI-	252	
A	C <sub>6</sub> H <sub>7</sub> O <sub>2</sub> NS	ESI-	156	
B	C <sub>6</sub> H <sub>4</sub> O <sub>2</sub>	ESI+	109	
C	C <sub>4</sub> H <sub>6</sub> ON <sub>2</sub>	/	98	
D	C <sub>4</sub> H <sub>6</sub> O <sub>2</sub> N <sub>2</sub>	ESI-	113	
E	C <sub>4</sub> H <sub>7</sub> O <sub>2</sub> N	ESI+	102	
F	C <sub>10</sub> H <sub>10</sub> O <sub>4</sub> N <sub>2</sub> S	ESI-	253	
G	C <sub>6</sub> H <sub>6</sub> O <sub>4</sub> S	/	174	
H	C <sub>10</sub> H <sub>9</sub> O <sub>5</sub> N <sub>3</sub> S	ESI-	282	
I	C <sub>10</sub> H <sub>11</sub> O <sub>5</sub> N <sub>3</sub> S	ESI+	274	
J	C <sub>7</sub> H <sub>7</sub> O <sub>5</sub> N <sub>3</sub> S	ESI+	246	

concentration of 20 mg l<sup>-1</sup>, initial pH 5.40). An approximately linear relationship between ln(C<sub>0</sub>/C<sub>t</sub>) and discharge time was observed ( $R^2 > 0.95$ ), which illustrates that the kinetics of degradation of SMX by the DBD plasma jet obeyed a quasi-first-order kinetic model. The degradation of SMX under the other treatment parameters discussed above in compliance with the quasi-first-order kinetic equation was also found, and the obtained degradation rate constants are shown in figure 8(b). The reaction rate constant of SMX degradation reached 1.06 min<sup>-1</sup> when oxygen was used as the working gas, and was

more than eight times higher than that when air was used as the working gas, and this is also the reason why we degraded SMX in water with oxygen plasma. The *k* value increased with decreasing initial concentration of SMX and increasing discharge power, and it also increased with decreasing initial pH of solution and reached 1.21 min<sup>-1</sup> at pH 3.04. However, the rate constant at the initial pH 5.40 of the solution has a high value of 88% compared to that at pH 3.04, and the environment of pH 5.40 does not require additional acid adjustment so as not to introduce other impurity ions. In addition, the environment of

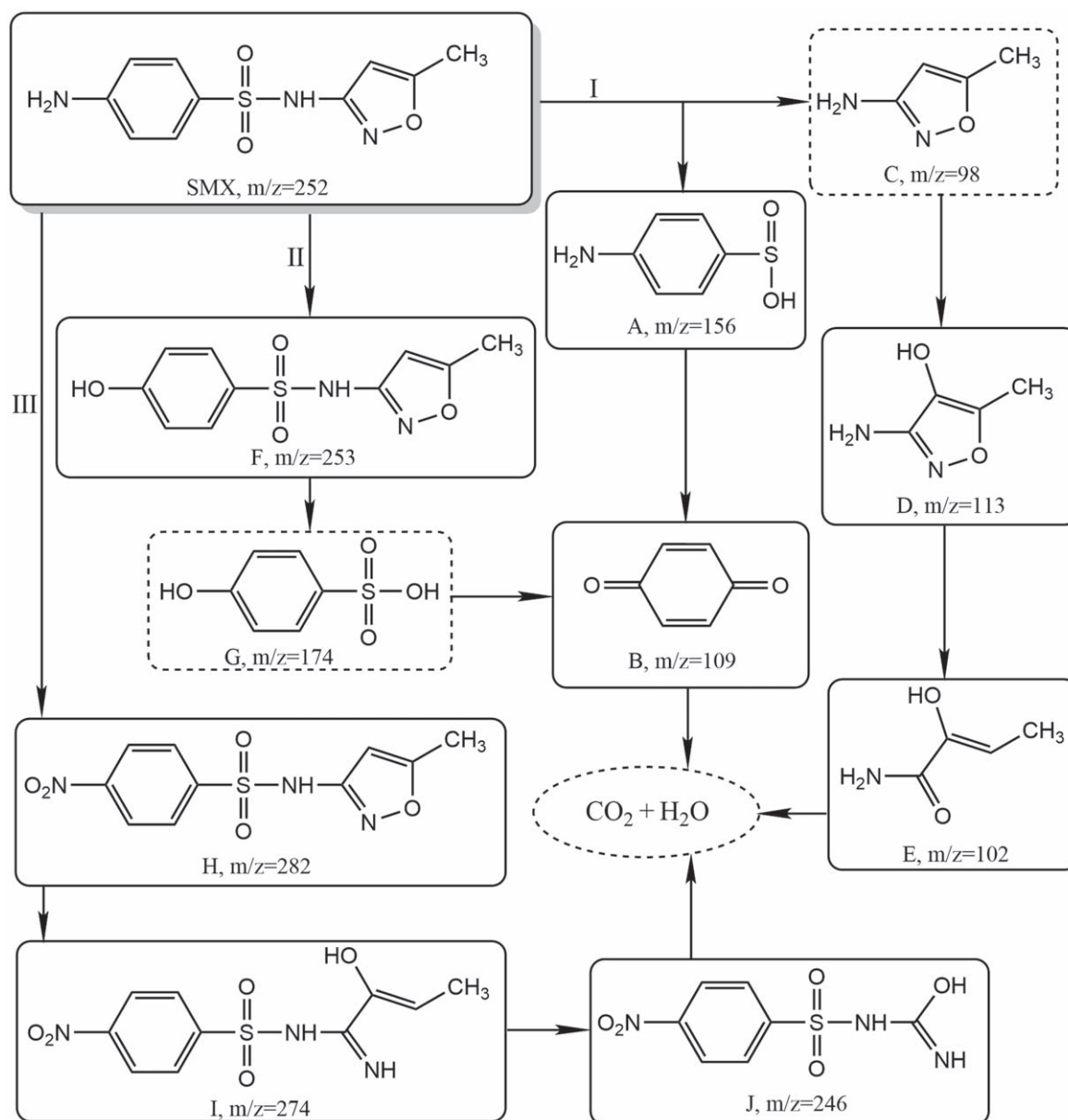


**Figure 10.** Proposed degradation pathways of SMX by the DBD plasma jet.

pH 5.40 is more moderate than that of pH 3.04, so we propose that the environment at pH 5.40 might be more suitable for this research.

**3.4.2. Extent of SMX mineralization.** Figure 9 displays the variation in TOC concentration during SMX degradation by the DBD plasma jet, and the extent of SMX mineralization in this system was obtained via the TOC removal rate. The SMX (initial concentration of  $20 \text{ mg l}^{-1}$ ) was almost completely degraded after 5 min of discharge treatment, but the mineralization rate only reached 26.15% at the same time. The mineralization rate was lower than the corresponding degradation efficiency of SMX, which indicated that some intermediate products would be generated in the degradation process. Extending the treatment time to 20 min, satisfactory

results appeared in that the mineralization rate reached 90.04%. A comparison of the removal rate of TOC during SMX degradation by different approaches was performed and is listed in table 1. Both gamma radiation/Fenton-like oxidation and peroxymonosulfate oxidation revealed relatively lower mineralization rates of 26.7% and 47.0%, respectively [54, 55]. Mineralization rates of 77.0% and 91.0% were achieved by electrochemical oxidation and UV/peroxydisulfate oxidation, but these two approaches were time-consuming [15, 56]. Moreover, Kim *et al* indicated that the mineralization rate of SMX degradation by a DBD plasma system reached only 24.3% [22]. The DBD plasma jet to degrade SMX could achieve a more desirable mineralization rate compared with these methods above. It is possible that there will be some differences in the final mineralization rate

due to the processing methods, processing parameters, initial concentration of the SMX, etc. However, based on the current results, our approach may still be a relatively ideal choice.

**3.4.3. Degradation intermediates and reaction pathways.** In order to fully understand the degradation mechanism of SMX by a DBD plasma jet, the degradation intermediates were identified by UPLC-MS. It is worth noting that the structures of the degradation intermediates were proposed according to the mass-to-charge ratio detected by UPLC-MS. The mass-to-charge ratios of intermediates and the corresponding deduced chemical formulas are listed in table 2. Based on the deduced chemical structures, the three probable pathways of SMX degradation by the DBD plasma jet are shown in figure 10. Pathway I describes the decomposition of SMX through the cleavage of the S–N bond, and this reaction is believed to be related to the attack of the S–N bond by reactive species such as hydroxyl radicals and ozone [57–59]. The cleavage of the S–N bond generates products 4-aminobenzenesulfonic acid and C, but the product C called 3-amino-5-methylisoxazole was not detected in this experiment, probably because the product C is easily further degraded by reactive species in a short period of time [60]. Further degradation of 4-aminobenzenesulfonic acid produces intermediate A called 4-aminobenzenesulfonic acid. The intermediate product A can be oxidized to intermediate B called benzoquinone. The isoxazole ring of intermediate C was attacked by hydroxyl radicals to form intermediate D with a hydroxylated structure. The intermediate product E could be attributed to the N–O bond cleavage of the isoxazole ring of intermediate D. Pathway II describes the decomposition of SMX through the attack of the hydroxyl radical; the amino group of the aniline ring of SMX was substituted by a hydroxyl group to generate intermediate F with a hydroxylated structure [61]. The S–N bond cleavage of intermediate F generates intermediates C and G, and the solubility of intermediate G in water may be too low to be detected in mass spectrometry experiments [62]. It can be clearly seen that an oxidation reaction occurred in pathway III; the amino group of the aniline ring of SMX was oxidized to generate the nitro compound H. When the isoxazole ring of intermediate H was attacked by hydroxyl radicals, not only was the N–O bond interrupted but a substitution reaction occurred to generate intermediate I with a hydroxylated structure, which could be further decomposed into intermediate J by demethylation. Eventually, some of the intermediates formed during SMX degradation by the DBD plasma jet were gradually mineralized into small inorganic molecules such as carbon dioxide and water.

**3.4.4. Toxicity evaluation.** Although SMX could be effectively removed from aqueous solution by the DBD plasma jet, a large number of intermediate products were formed in this process. Thus, it is necessary to assess the potential risk of SMX and its intermediate products to the environment; the aquatic toxicity was evaluated through the growth inhibition experiment of *E. coli* in this research

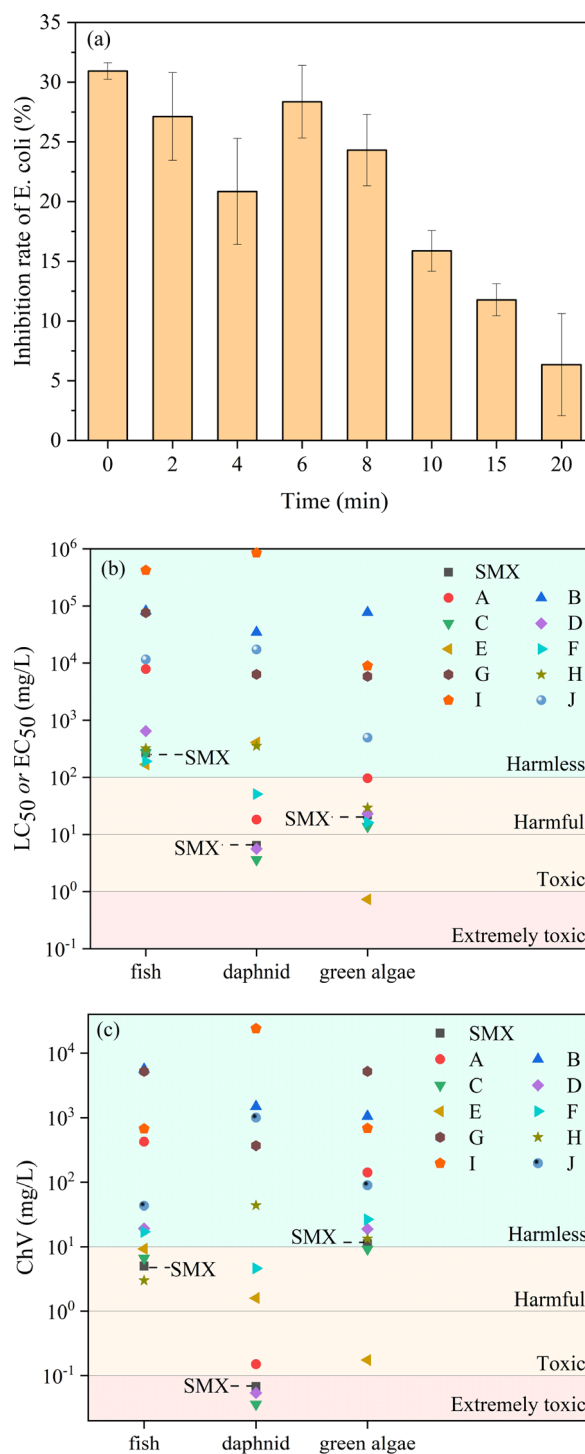


**Figure 11.** Toxicity assessment. (a) *E. coli* growth inhibition rate, (b) acute toxicity, (c) chronic toxicity. (European Union standard for acute toxicity, harmless ( $>100 \text{ mg l}^{-1}$ ), harmful ( $10\text{--}100 \text{ mg l}^{-1}$ ), toxic ( $1\text{--}10 \text{ mg l}^{-1}$ ) and extremely toxic ( $<1 \text{ mg l}^{-1}$ ); Chinese hazard chemical evaluation guidelines for chronic toxicity (HJ/TI 154–2004), harmless ( $>10 \text{ mg l}^{-1}$ ), harmful ( $1\text{--}10 \text{ mg l}^{-1}$ ), toxic ( $0.1\text{--}1 \text{ mg l}^{-1}$ ) and extremely toxic ( $<0.1 \text{ mg l}^{-1}$ ).

(figure 11(a)). As the SMX was degraded gradually with the plasma treatment time, the degradation efficiency of SMX reached 97% after 4 min treatment, and the aquatic toxicity decreased to 20.85%. However, a rise in toxicity was observed from 4 min to 6 min, reaching a greater inhibition

rate of 28.36% by 6 min, which may be explained by the higher toxicity of the small molecule intermediate products produced. Therefore, the acute toxicity and chronic toxicity of SMX and its degradation intermediates to fish, daphnia, and green algae were predicted by the ECOSAR program [63, 64]. It could be seen that SMX exhibits high toxicity to several of these organisms, especially to daphnia (figures 11(b) and (c)). Intermediate products A and C show similar toxicity to the parent SMX. However, intermediate E shows higher acute and chronic toxicity to green algae than the parent SMX and other intermediates, which most likely contribute to the inhibition rate in the *E. coli* inhibition experiment rising again after plasma treatment for 6 min. With increasing treatment time, these intermediates were further degraded into harmless compounds such as intermediates B and G, and the inhibition rate of *E. coli* reached a minimum value of 6.34% after 20 min treatment. In summary, SMX was gradually degraded and mineralized by the DBD plasma jet, which eventually resulted in a lower toxicity of the aqueous solution.

#### 4. Conclusion

In this research, the degradation of SMX in aqueous solution using a DBD plasma jet was investigated. The experimental results indicate that the degradation efficiency of SMX was higher at an oxygen atmosphere, higher discharge power, lower initial SMX concentration, and acidic environment. Reactive species detection experiments substantiated that OH radicals and O<sub>3</sub> played a significant role in SMX degradation, while H<sub>2</sub>O<sub>2</sub> did not. Kinetic analysis showed that the process of the SMX degradation obeyed the quasi-first-order kinetic equation, and the high mineralization rate of SMX degradation indicated that DBD plasma jet is a highly efficient method for removing pollutants in aqueous solution. The intermediate products of SMX degradation were analyzed by UPLC-MS to propose the possible degradation pathways, which included cleavage of the S–C bond, deamination of the aniline ring, oxidation of the amino group, and hydroxylation of the isoxazole ring and aniline ring. Toxicity analysis indicated that although the value of aquatic toxicity fluctuated, solution toxicity decreased to a lower level with longer plasma treatment time. In summary, a DBD plasma jet is a green and efficient method to degrade SMX in aqueous solution, which provides support for its application in the field of degradation of refractory organic pollutants.

#### Acknowledgments

This work was supported jointly by National Natural Science Foundation of China (Nos. U20A20372, 51807046, 51777206) and the Natural Science Foundation of Anhui Province (Nos. 2108085MD136, 1908085MA29).

#### References

- [1] Burkhardt-Holm P 2010 *Int. J. Water Resour. Dev.* **26** 477
- [2] Hama Aziz K H et al 2017 *Chem. Eng. J.* **313** 1033
- [3] Barrios-Estrada C et al 2018 *Sci. Total Environ.* **612** 1516
- [4] Kwon B et al 2016 *Environ. Toxicol. Pharmacol.* **48** 168
- [5] Zhang Q Q et al 2015 *Environ. Sci. Technol.* **49** 6772
- [6] Lach J et al 2018 *Problemy Ekorozwoju* **13** 197
- [7] Li S et al 2018 *J. Environ. Manage.* **228** 65
- [8] Chen Y et al 2017 *Chemosphere* **180** 467
- [9] Hanna N et al 2020 *Int. J. Environ. Res. Public Health* **17** 7706
- [10] Sabri N A et al 2020 *J. Environ. Chem. Eng.* **8** 102245
- [11] Rosal R et al 2010 *Water Res.* **44** 578
- [12] Sahar E et al 2011 *Water Res.* **45** 4827
- [13] Chen H and Wang J 2021 *J. Hazard. Mater.* **407** 124377
- [14] Zhang H et al 2021 *Mater. Today Commun.* **27** 102288
- [15] Ganiyu S O et al 2018 *Chem. Eng. J.* **350** 84
- [16] Xu Z et al 2018 *Bioelectrochemistry* **121** 125
- [17] Cheng C et al 2006 *Surf. Coat. Technol.* **200** 6659
- [18] Xu Z et al 2022 *Chem. Eng. J.* **429** 132397
- [19] Tang S et al 2018 *J. Environ. Manage.* **226** 22
- [20] Jiang N et al 2018 *Chem. Eng. J.* **350** 12
- [21] Hu X and Wang B 2021 *J. Environ. Chem. Eng.* **9** 105720
- [22] Kim K-S et al 2015 *Chem. Eng. J.* **271** 31
- [23] Deng R et al 2021 *Chem. Eng. J.* **406** 126884
- [24] Liu Y et al 2018 *Chem. Eng. J.* **345** 679
- [25] Chandana L et al 2015 *Chem. Eng. J.* **282** 116
- [26] Rashid M M et al 2020 *J. Environ. Chem. Eng.* **8** 104504
- [27] Xu Z et al 2021 *Plasma Process. Polym.* **19** e2100122
- [28] Magureanu M et al 2015 *Water Res.* **81** 124
- [29] Shiraki D et al 2016 *IEEE Trans. Plasma Sci.* **44** 3158
- [30] Mirzaei A et al 2021 *Chem. Eng. J.* **422** 130507
- [31] Shen J et al 2019 *Chem. Eng. J.* **362** 402
- [32] Lukes P and Locke B R 2005 *J. Phys. D-Appl. Phys.* **38** 4074
- [33] Knipping E M 2002 *J. Geophys. Res.* **107** 4360
- [34] Xu Z et al 2020 *Sep. Purif. Technol.* **230** 115862
- [35] Chen G et al 2009 *J. Hazard. Mater.* **172** 786
- [36] Ao X et al 2021 *Water Res.* **203** 117458
- [37] Jiang B et al 2012 *Chem. Eng. J.* **204–206** 32
- [38] Wang T et al 2016 *Water Res.* **89** 28
- [39] Wu J et al 2020 *Chem. Eng. J.* **384** 123300
- [40] Milh H et al 2021 *Chem. Eng. J.* **422** 130457
- [41] Liu Y et al 2016 *Water Res.* **95** 195
- [42] Guo Z et al 2015 *Environ. Sci. Pollut. Res.* **22** 15772
- [43] Sayed M et al 2016 *Environ. Technol.* **37** 590
- [44] Zhang Z et al 2017 *Plasma Chem. Plasma Process.* **37** 415
- [45] Gao L et al 2020 *Environ. Pollut.* **259** 113795
- [46] Amina et al 2018 *Chem. Eng. J.* **353** 80
- [47] Du J et al 2018 *Water Res.* **138** 323
- [48] Nikiforov A Y et al 2011 *Plasma Sources Sci. Technol.* **20** 015014
- [49] Kanazawa S et al 2011 *Plasma Sources Sci. Technol.* **20** 034010
- [50] di Luca C et al 2021 *Chem. Eng. J.* **412** 128579
- [51] Chen Z et al 2019 *Plasma Sources Sci. Technol.* **28** 025001
- [52] van Gils C A J et al 2013 *J. Phys. D-Appl. Phys.* **46** 175203
- [53] Park S et al 2019 *Chem. Eng. J.* **378** 122163
- [54] Zhuan R and Wang J 2020 *Radiat. Phys. Chem.* **166** 108457
- [55] Gong H et al 2020 *Chem. Eng. J.* **389** 124084
- [56] Yan S et al 2021 *Sep. Purif. Technol.* **274** 118991
- [57] Wang L et al 2016 *Water Res.* **88** 322
- [58] Song Y et al 2021 *Chemosphere* **269** 128684
- [59] Huang Y and Yang J 2022 *Sci. Total Environ.* **803** 150074
- [60] Xie Y et al 2022 *Chem. Eng. J.* **429** 132237
- [61] Wang A et al 2011 *Appl. Catal. B-Environ.* **102** 378
- [62] Shen J H et al 2021 *J. Colloid Interface Sci.* **586** 563
- [63] Chen H and Wang J 2021 *J. Hazard. Mater.* **403** 123697
- [64] Yang J et al 2020 *Int. J. Mol. Sci.* **21** 6276